

A Tunable EBG Absorber for Radio-Frequency Power Imaging

*Satoshi Yagitani¹, Keigo Katsuda¹, Ryo Tanaka¹, Masayuki Nojima¹,
Yoshiyuki Yoshimura², and Hirokazu Sugiura²*

¹Graduate School of Natural Science and Technology, Kanazawa University,
Kakuma-machi, Kanazawa 920-1192, Japan
E-mail: yagitani@reg.is.t.kanazawa-u.ac.jp

²Industrial Research Institute of Ishikawa, 2-1 Kuratsuki, Kanazawa 920-8203, Japan

Abstract

Absorption characteristics of a tunable electromagnetic band-gap (EBG) absorber are analyzed, which is designed to capture 2d radio-frequency (RF) power distributions incident on the absorber surface. The EBG absorber has lumped resistors interconnecting the mushroom-type surface patches to absorb the incident RF power at the resonance frequency where the EBG structure exhibits a high-impedance feature. The absorbed RF power distribution is measured by directly detecting the amounts of RF power consumed by the individual resistors. Varactor diodes are inserted in parallel with the resistors for tuning the resonance frequency of narrowband absorption. The absorption characteristics at normal incidence are evaluated in detail based on an equivalent circuit model which exactly explains the frequency behavior of the surface impedance of the tunable EBG absorber observed in EM simulation. The small resistance existing in the varactor diode makes it difficult for the surface impedance to be matched with the incident wave impedance (*i.e.*, for a high absorption to be achieved) over a wide range of resonance frequency. A means to improve the absorption performance of the tunable EBG absorber is examined.

1. Introduction

A variety of thin electromagnetic absorbers have been designed based on the artificial high-impedance surfaces such as frequency-selective surfaces and metamaterial surfaces (*e.g.*, [1] and references therein). At the resonance frequency where these surfaces exhibit the high-impedance feature, an incident wave is absorbed by the additional resistive components which are matched with the incident wave impedance. Recently it was proposed that a thin absorber can be used for monitoring 2d radio-frequency (RF) power distributions incident on the absorber surface [2]. A mushroom-type electromagnetic band-gap (EBG) structure is used as the high-impedance surface, where the absorption is achieved by “lumped resistors” connecting between the adjacent patches on the mushroom layer [3]. With this configuration the power of an RF wave incident on the mushroom surface is absorbed (or consumed) by the lumped resistors. By directly measuring the power consumption in each of the lumped resistors arranged in a 2-d matrix, the 2-d distribution of the RF power incident and absorbed on the mushroom surface is obtained. Such an “RF power imager” has inherently a narrowband feature around the resonance frequency fixed by the geometrical and constitutional structure of the EBG surface. To extend the measurable frequency range, the resonance frequency is made electronically tunable by additional varactor diodes (varactors), as in [4-5]. A 347-mm square EBG absorber was designed and fabricated to cover the absorbing frequency range from 700 MHz up to 2.7 GHz. Power distributions were detected at 8×8 locations on the absorber, at each of which two RF power detectors with the sensitivity of -70 dBm were placed to measure two orthogonal polarizations. The measured power distributions were transferred to a PC and displayed as real-time 2-d power images at a rate of 30 images/second. The RF power distributions radiated from a dipole antenna were measured to be consistent with those expected theoretically, which validated the proposed technique to measure the RF power distributions. Using such an RF power imager, the power distributions of even impulsive RF signals and/or noises can be captured and visualized in situ and in real-time, while the electromagnetic environment is almost undisturbed by the EBG absorber.

In the present study, the absorption characteristics of the tunable EBG absorber designed for RF power imaging is evaluated in detail based on equivalent circuit analysis and EM simulation.

2. A Tunable EBG Absorber for Detecting RF Power Distribution

Figure 1 shows the geometrical structure of a square unit cell of the tunable EBG absorber designed for RF

power imaging, which has lumped resistors and varactors inserted between the adjacent patches on the surface [2]. The gap g between the adjacent patches is much smaller than the patch size w , and the periodicity of the unit cells, $a = w + g$, is set much smaller than the wavelength. For an electromagnetic wave at normal incidence, the surface impedance of the mushroom structure itself is represented as a parallel connection of the effective inductance and capacitance. The high-impedance feature is achieved at the LC resonance frequency, where the mushroom layer behaves like an artificial magnetic conductor. The incident wave power is absorbed by the lumped resistors interconnecting the surface patches; if we take the value of the resistors as $R = 377 \Omega$ matched with the incident wave impedance, the incident wave should be completely absorbed at the resonance frequency [3]. On the other hand, tunability is achieved by the varactors inserted in parallel with the resistors, by altering the capacitance component of the EBG structure which specifies the resonance frequency. As in the same manner designed by [6], the varactors are oriented in opposite directions in each alternate row as well as in each alternate column of the matrix of mushrooms. Reverse biases are supplied to all the varactors by alternately biasing half of the cells, and grounding the other half in a checkerboard pattern (see Fig. 3 of [6]). A separate biasing circuit is placed on the backside of the ground plane. Thus, by applying appropriate bias voltages to the varactors, we can control the frequency of RF power absorption. The locations of the varactor and the resistor, as well as their separation distance d , on each side of a patch has an effect on the surface impedance, as discussed in Sec. 3.

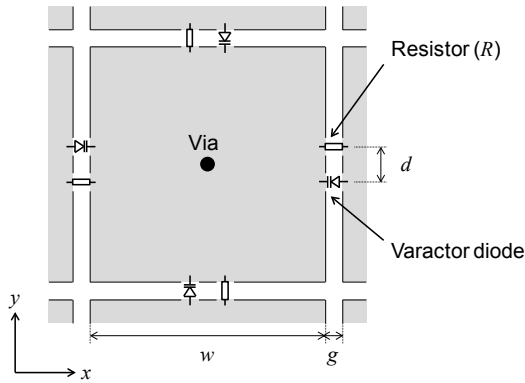


Fig. 1: Structure of a unit cell of the EBG absorber

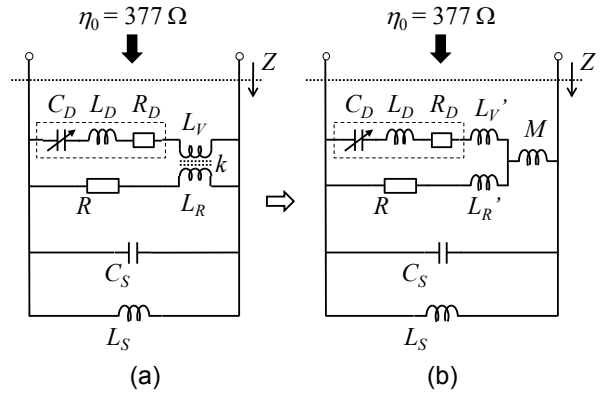


Fig. 2: Equivalent circuit model

On the EBG absorber in Fig. 1, the incident wave power is absorbed and dissipated in the surface resistors, when there are no losses in the varactors and in the substrate. The amount of power absorbed by each resistor depends on the incident polarization; the resistors connecting the adjacent patches in the x - and y -directions absorb the amounts of RF power with the electric field polarized in the x - and y -directions, respectively [2]. In either case, the power absorbed by each resistor is considered to be the Poynting flux of the incident wave multiplied by the area of a unit cell. By detecting directly the amounts of power consumed in the 2-d matrix of surface resistors, the 2-d power distribution of the RF wave illuminating the EBG surface is measured with polarization discrimination. Power detectors are put on the backside of the EBG absorber, to detect the amounts of power consumed by the individual surface resistors [2].

3. Equivalent Circuit Analysis

Here the characteristics of the tunable EBG absorber shown in Fig. 1 are evaluated. The geometrical and constitutional parameters are similar to those of the EBG absorber designed in [2], which had 33×33 square unit cells formed on an FR-4 substrate of 347 mm square and 1.6 mm thick. The size of a patch is $w = 10$ mm and the gap between the adjacent patches is $g = 0.5$ mm, so that the cell periodicity is $a = 10.5$ mm. The via diameter is 0.6 mm. The relative permittivity of the FR-4 substrate is taken as 4.56 with no loss ($\tan\delta = 0$). The varactor is modeled as a series RLC circuit; the series resistance $R_D = 1 \Omega$, the parasitic inductance $L_D = 1.8$ nH and the capacitance C_D is variable from 0.67 to 12 pF (which makes the absorber tunable from 700 MHz to 2.7 GHz). It is noted that the resistor was chosen here as $R = 845 \Omega$ instead of 377Ω , to have maximum absorption at 2 GHz (see the discussion in the next paragraph). Using these parameters, the absorption characteristics of the EBG absorber were computed by an EM simulator (CST Microwave Studio). A linearly polarized plane wave was incident normally on the EBG surface. A square area containing four unit cells of the absorber was modeled by defining the periodic boundary condition, which corresponds to simulating infinitely extending periodic unit cells.

The equivalent circuit which exactly reproduces the absorption characteristics obtained in the simulation is shown in Fig. 2 (a). The effective capacitance and inductance of the mushroom structure are $C_S = 0.628$ pF and $L_S = 1.86$ nH, respectively. The effects of the surface currents on a patch flowing toward the varactor (C_D , L_D and R_D) and the resistor (R) are represented by a transformer, L_V and L_R coupled with the coefficient k , which are dependent of the geometrical configuration of the varactor and the resistor on each side of the patch (*i.e.*, their locations as well as their separation distance d). The parameters of the transformer can be replaced with L_V' , L_R' and their mutual inductance M as in Fig. 2 (b); for the case of $d = 1$ mm, $L_V' = 0.371$ nH, $L_R' = 0.41$ nH and $M = 0.235$ nH. From this circuit, two resonance frequencies are derived by solving Eq. (1) for ω .

$$\frac{\omega^4}{\omega_S^2 \omega_D^2} - \left(\frac{1}{\omega_S^2} + \frac{1}{\omega_D^2} + \frac{1}{\omega_C^2} \right) \omega^2 + 1 = 0, \text{ where } \omega_S = (L_S C_S)^{-1/2}, \quad \omega_D = \left[(L_D + L_V' + M) C_D \right]^{-1/2}, \quad \omega_C = (L_S C_D)^{-1/2}. \quad (1)$$

The surface impedance Z of the EBG absorber becomes purely resistive R_p at each resonance frequency, and the reflection coefficient is given as $\Gamma = (R_p - \eta_0) / (R_p + \eta_0)$, where $\eta_0 = 377 \Omega$ is the incident wave impedance. When the capacitance of the varactor C_D is varied, the resonance frequencies are changed accordingly. The value of the resistance R_p at the resonance frequency ω_r is calculated as

$$R_p = \frac{Z_S^2}{R_D} \left(\frac{\omega_r}{\omega_S} - \frac{\omega_S}{\omega_r} \right)^{-2} // \left[R \left(\frac{1}{1 + (1 - \omega_r^2 / \omega_S^2) M / L_S} \right)^2 \right], \text{ where } Z_S = (L_S / C_S)^{1/2}, \quad (2)$$

where $//$ means the parallel connection of the impedance. The typical frequency variation of the surface impedance under the circuit parameters mentioned above is shown in Fig. 3. The absolute value of surface impedance $|Z|$ is shown by the solid line for the case of $C_D = 1.35$ pF. In this case the first and second resonance frequencies appear at 2.0 GHz and 6.7 GHz, respectively, which are observed as the two peaks on $|Z|$. When C_D is varied from 12 pF down to 0.67 pF, the first resonance frequency is changed from 700 MHz up to 2.7 GHz, whereas the second one is from 6.23 GHz up to 6.85 GHz. Over each resonance frequency range, the value of the resistance moves on the broken curve specified by Eq. (2). From the viewpoint of achieving frequency tunability, the first resonance should be taken, as the variable range of the second resonance frequency is unpractically narrow. To achieve a high absorption at each resonance frequency, the resistance should be as close as possible to the incident wave impedance, $\eta_0 = 377 \Omega$ (the dotted line). From Eq. (2), R_p becomes equal to R at $\omega_r = \omega_S$, and $R_p \sim (Z_S^2 / R_D) (\omega_r / \omega_S)^2 // [R / (1 + M / L_S)^2]$ for $\omega_r \ll \omega_S$; the surface resistance becomes smaller as the resonance frequency becomes lower. Thus the existence of the small resistance R_D in the varactor has a considerable effect on the frequency behavior of the surface impedance [4]. Here $\omega_S / 2\pi = 4.66$ GHz and $Z_S^2 / R_D = 2.96$ k Ω , and R was chosen as 845 Ω so that R_p becomes 377 Ω at 2.0 GHz. Above and below 2.0 GHz, R_p becomes larger and smaller than 377 Ω , respectively, leading to impedance mismatch in either case.

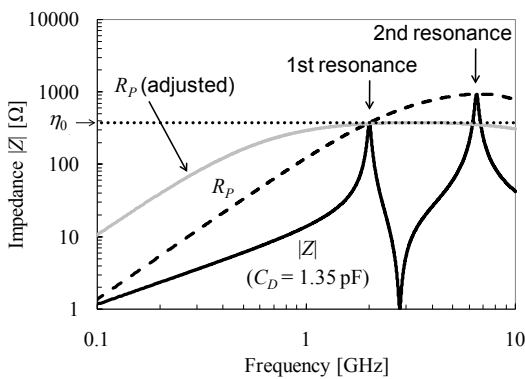


Fig. 3: Surface impedance of the EBG absorber

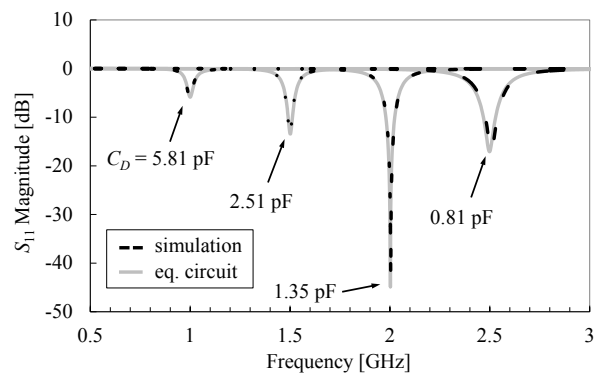


Fig. 4: Reflection magnitude of the EBG absorber

Figure 4 shows the reflection magnitude profiles for the first resonance obtained by the equivalent circuit analysis and the simulation, which are plotted by gray and dotted lines, respectively. In each case four representative profiles are plotted for the varactor capacitances fixed as $C_D = 5.81$ pF, 2.51 pF, 1.35 pF and 0.81 pF, which correspond to the resonance frequencies of 1.0 GHz, 1.5 GHz, 2.0 GHz and 2.5 GHz, respectively. For each of the capacitance values, the reflection profile calculated by the equivalent circuit analysis agrees well to that observed in the simulation,

which validates the accuracy of the equivalent circuit in Fig. 2. Also for the second resonance, though not shown here, a good agreement was observed between the reflection profiles obtained by the equivalent circuit analysis and in the simulation. On each curve, the reflection becomes minimum (the absorption becomes maximum) at the resonance frequency determined by the value of C_D . As discussed above, the amount of absorption becomes highest ($S_{11} \sim -45$ dB) at the resonance frequency of 2.0 GHz for the case of $C_D = 1.35$ pF, where the surface impedance of the EBG absorber R_S becomes 377Ω . When the resonance frequency goes above or below 2.0 GHz, the maximum absorption is degraded due to the increase in mismatch between R_S and 377Ω .

As discussed above, Eq. (2) is approximated as $R_p \sim (Z_S^2/R_D) (\omega_r/\omega_S)^2 // [R/(1+M/L_S)^2]$ at first resonance frequencies $\omega_r \ll \omega_S$. If the three conditions, $(Z_S^2/R_D) (\omega_r/\omega_S)^2 \gg R$, $R = 377 \Omega$ and $M \ll L_S$, are satisfied, $R_p \sim 377 \Omega$ so that a high absorption would be achieved over a certain range of resonance frequency. Since the first condition is rewritten as $\omega_r^2 L_S^2 / R_D \gg R$, one way to make it so is to use the varactor with the resistance R_D as small as possible. The other is to increase the effective inductance L_S by increasing the thickness of the substrate. The gray line in Fig. 3 shows the surface resistance profile expected for the case of $R_D = 0.5 \Omega$, $R = 377 \Omega$, $L_S = 3.72$ nH (corresponding to the substrate thickness of 3.2 mm) and $M = 0$ nH (which is achievable by adjusting the distance d between the resistor and the varactor). In this case $R_p \sim 377 \Omega$ is achieved over a wide range of resonance frequency above 1 GHz.

4. Conclusion

Absorption characteristics of the tunable EBG absorber used for imaging the RF power distributions were evaluated by the equivalent circuit analysis and the simulation. A realistic equivalent circuit model was derived which exactly explains the frequency behavior of the surface impedance of the EBG absorber for normal incidence observed in the simulation. It was shown that the small resistance existing in the varactor diode makes it difficult for the surface impedance to be matched with the incident wave impedance over a wide range of resonance frequency. A means to improve the absorption performance of the tunable EBG absorber was examined. Evaluation for oblique incidence will be the future work.

Acknowledgments

The authors would like to thank Dr. M. Ozaki for his valuable suggestions and discussions. This study was supported by KAKENHI (21560444).

References

1. F. Costa, A. Monorchio, G. Manara, "Analysis and design of ultra thin electromagnetic absorbers comprising resistively loaded high impedance surfaces," *IEEE Trans. Antennas and Propagation*, **58**, 5, May 2010, pp.1551–1558.
2. S. Yagitani, K. Katsuda, M. Nojima, Y. Yoshimura, and H. Sugiura, "Imaging Radio-Frequency Power Distributions by an EBG Absorber," *IEICE Trans. Commun.*, 2011, submitted.
3. Q. Gao, Y. Yin, D.-B. Yan, and N.-C. Yuan, "A novel radar-absorbing-material based on EBG structure," *Microwave and Optical Technology Letters*, **47**, 3, Nov. 2005, pp.228–230.
4. C. Mias, and J. H. Yap, "A varactor-tunable high impedance surface with a resistive-lumped-element biasing grid," *IEEE Trans. Antennas and Propagation*, **55**, 7, July 2007, pp.1955–1962.
5. R. Miyazaki, A. Nishikata, T. Aoyagi, and Y. Kotsuka, "Tunable EM-wave absorber below 1 GHz using diode grid and its evaluation by large stripline," *Proc. 2009 International Symposium on Electromagnetic Compatibility*, July 2009, pp.729–732.
6. D. F. Sievenpiper, J. H. Schaffner, H. J. Song, R. Y. Loo, and G. Tansonan, "Two-dimensional beam steering using an electrically tunable impedance surface," *IEEE Trans. Antennas and Propagation*, **51**, 10, Oct. 2003, pp.2713–2722.